Local Order and Induced Orientation in PDMS Model Networks, Studied by ^{2}H NMR

P. Sotta

Laboratoire de Physique des Solides (CNRS-LA0002), Université Paris-Sud, bât. 510, 91405 Orsay Cedex, France

Received July 8, 1997; Revised Manuscript Received October 2, 1997

ABSTRACT: ^{2}H NMR experiments in a series of poly(dimethylsiloxane) end-linked networks are presented. The ^{2}H NMR line shape in the relaxed state consists of a pseudo-solid contribution, with nonzero residual interactions, and a liquid contribution, with no residual interactions. The liquid part is attributed to dangling chains. The magnitude of residual interactions in the pseudo-solid part (elastic chains) is compared to the magnitude of the uniaxial order induced upon stretching uniaxially the networks. The induced order is measured by the splitting of the doublet which appears upon stretching. The splitting correlates also well with the polymer network volume fraction at swelling equilibrium. All these quantities are related to the properties of effectively elastic chains in the networks. The presence of dangling chains does not modify the interpretation given previously for the induced uniaxial order, in terms of a mean orientational field. The analysis which is presented allows one to estimate the strength of orientational interactions between segments.

1. Introduction

Rubbers and gels are important materials for numerous and important applications.[1−4] Nuclear magnetic resonance (NMR) allows one to relate macroscopic properties (such as elastic moduli, birefringence induced under strain, or equilibrium swelling) to the microscopic behavior of polymer chains.[5,6] One essential NMR property in such systems is the presence of residual interactions, due to the local order related to the constraints exerted on polymer chains by cross-link junctions.[7−13]

A number of deuterium (^{2}H) NMR studies in end-linked poly(dimethylsiloxane) (PDMS) model networks have been already performed.[14−24] The molecular orientation induced by a uniaxial strain was studied in details. It was shown that it may be interpreted in terms of short-range orientational (nematic-like) interactions between segments.[20] On the other hand, residual interactions in the relaxed network have been analyzed. It was shown that dangling chains have an NMR behavior which is different from that of elastic chains, leading to a two-component NMR signal.[24] The induced orientation and the residual interactions in the relaxed state, being both related to elastic properties of chains, are expected to depend on the same molecular parameters. Though all these quantities have been measured and correlated in several series of PDMS networks, the number values were not compared directly. Therefore we propose here to correlate quantitatively both quantities. We show that this comparison allows one to estimating the parameter u which characterizes the strength of short-range orientational interactions between segments.[20] To do so, the NMR signal has to be analyzed carefully. The signal from network chains has a liquidlike component, which behaves isotropically in the relaxed state. This component in the signal is attributed to dangling chains. The estimate of the parameter u is coherent with those previously published, provided that dangling chains are properly taken into account. The presence of a fraction of chains with a liquidlike behavior does not preclude the mean-field model for the induced order which was proposed in previous works.

The paper is organized as follows. First, we recall the basics about ^{2}H NMR in polymer networks, and a basic (Gaussian) model widely used to analyze these experiments (section 2). In section 3, we describe the series of PDMS networks which have been used. Experimental results are presented in section 4. First, the orientation induced upon stretching is correlated to the equilibrium swelling. This was already done in refs 15 and 16 to show that the induced order is sensitive to the number of trapped entanglements. Here a quantitative comparison within the framework of the Gaussian model mentionned above gives an estimate of the interaction parameter u. Then it is shown that the half-height line width of the spectra does not correlate well to the magnitude of the orientational order induced by stretching. The line shape is then analyzed more precisely, to separate the contribution from dangling chains. Results are discussed in Section 5.

2. ^{2}H NMR Properties of Networks

2.1. Residual Quadrupolar Interactions. ^{2}H NMR properties are determined by the way in which the quadrupolar Hamiltonian $H_Q(t) = (\omega_Q/3)P_2(\theta(t))(3I_z^2 - 2)$ is averaged by molecular motions.[25−26] The space variable of the interaction is the angle $\theta(t)$ between the quadrupolar tensor and the magnetic field ($P_2(\theta)$ is the second-order Legendre polynomial $P_2(\theta) = (3\cos^2\theta - 1)/2$). ω_Q is the quadrupolar coupling constant ($\omega_Q = 2\pi \times 125$ kHz).

It was shown long ago that elastic chains are characterized by the presence of residual interactions due to motional restrictions, related to cross-link junctions.[7,8,27,28] In the limit of fast intrachain motions, the residual interaction within one elastic chain is [8,20]

$$\Delta_R = \frac{3}{5}\omega_Q \frac{R^2}{N^2a^2}P_2(\alpha) = \frac{3}{10}\omega_Q\frac{1}{N^2a^2}(2z^2 - x^2 - y^2) \quad (1)$$

(R,α) (respectively (x,y,z)) are the polar (respectively

S0024-9297(97)00994-7 CCC: $15.00
Published on Web 05/23/1998

Table 1. Characteristics of Monomodal Networks[a]

refs	M_n(D)	M_n(H)	Φ_D	ν_C	f	w_f	w_p
G3	3100	3050	0.19	0.7	4	0.004	0.12
G19	10500	9900	0.2	0.7	4	0.004	0.12
G21	10500	9900	0.19	1	4	0.003	0.1
G26	23000	25000	0.09	1	4	0.0065	0.15
G27	23000	25000	0.19	0.7	4	0.017	0.23
G30	10500	9700	0.19	1	6	0.0023	0.09
G31	10500	9700	0.27	0.7	6	0.0065	0.15
G32	23000	25000	0.07	1	6	0.008	0.16
H21*	9700	10500	0.15	1	4 (1)	0.01	0.18

[a] Key: M_n(D), number average molecular mass of deuterated precursor chains; M_n(H), id for hydrogenated precursor chains; Φ_D, fraction of deuterated chains; v_c, polymer concentration in the cross-linking reaction bath; f, functionality of junctions; w_f, fraction of functional precursor polymer chains extracted after the cross-linking reaction; w_p, fraction of dangling chains, estimated from w_f.

Cartesian) coordinates of the chain end-to-end vector, in a fixed frame with axis z along the magnetic field $\vec{B}_0$. a is a typical monomer length. Elastic chains are described here as freely jointed chains of N segments, terminated by junctions which are fixed in space on average. Each segment has a quadrupolar tensor directed along the segment.

For a PDMS chain, one has to take into account fast molecular motions inside a monomer, which average the quadrupolar interaction along the chain tangent. In $-CD_3$ groups, the quadrupolar tensor is uniaxial, directed along the C−D bond. Thus, fast rotation around $-CD_3$ group axis average the interaction along this axis, with a reduction factor of $^1/_3$. Then, rotation of the monomer around the O−O axis further averages the interaction along the local chain direction, with an additional reduction factor of $^1/_2$. Thus it is convenient to consider that the interaction is reduced by a factor of $^1/_6$ and to use the effective value $\omega_Q = 2\pi 125/6 = 2\pi \times 21$ kHz.

For an elastic chain (or chain fragment), the relaxation function is

$$M(t) = M_0 \exp\left(-\frac{t}{T_2}\right)\cos(\Delta_R t) \qquad (2)$$

In a network made of chains (or chain fragments) with a Gaussian distribution $P(\vec{R})\,d\vec{R} = (\sigma^2/\pi)^{3/2}\exp(-\sigma^2 R^2)\,d\vec{R}$ (with $\sigma^2 = 3/2Na^2$)), the overall relaxation function is,[5,9] neglecting the irreversible term $\exp[-t/T_2]$:

$$M(t) = M_0\,\mathrm{Re}\left[\left(1 - i\frac{2}{5}\frac{\omega_Q t}{N}\right)^{-1/2}\left(1 + i\frac{1}{5}\frac{\omega_Q t}{N}\right)^{-1}\right] \qquad (3)$$

This function describes the behavior of the elastic part of the network. In this very simple model, it is related to the molecular properties of the network through one single parameter, namely the effective average chain length N.

2.2. Splitting in a Uniaxially Stretched Network. In a uniaxially stretched network, the resonance spectrum is splitted into a doublet. This doublet is due to the presence of a mean orientational field, which was interpreted as the effect of short-range orientational interactions between chain segments.[18−20] The splitting (measured in Hz) is given by[20]

$$\Delta\nu = \frac{2}{5}\frac{\nu_Q}{N}\frac{u}{1-u}|P_2(\Omega)|(\lambda^2 - \lambda^{-1}) \qquad (4)$$

in which $\nu_Q = \omega_Q/2\pi = 21$ kHz and $\lambda = L/L_0$ is the elongation ratio. Ω is the angle between the applied uniaxial force $\vec{F}$ and the magnetic field $\vec{B}_0$. The quantity which is measured is the slope $P = \Delta\nu/(\lambda^2 - \lambda^{-1})$. The parameter u characterizes the strength (in k_BT units) of the segmental interactions.[20] The value of u should be comprised between 0 and 1. The value u=1 would correspond in this model to a spontaneous nematic transition (i.e. to a nonzero orientation for $\lambda \neq 1$).

3. Experimental Section

3.1. Samples. Dry PDMS networks were used. They were obtained by end-to-end cross-linking, as described in refs 29 and 30. First, a series of monomodal networks was studied. The characteristics are summarized in Table 1. The index of polydispersity of precursor chains is 1.6. A fraction Φ_D of the precursor chains are perdeuterated. The cross-linking agent for tetrafunctional networks ($f = 4$) is tetrakis(allyloxyethane), except for network H21 which has cyclic cross-links made from tetrakis(vinylcyclosiloxane) (TVCS). Hexafunctional networks ($f = 6$) are cross-linked with bis(allyloxy-3-diallyloxymethyl-2,2-propyl oxide). The cross-linking reaction was performed either in the bulk or in concentrated solution (concentration $\nu_c \geq 0.5$), with stoichiometric amounts of cross-linking agent. w_f is the fraction of functional precursor chains extracted after cross-linking (relative to the total precursor polymer). w_f is measured from a GPC analysis of the extractible products, which contain also nonfunctional oligomers (typically 4% of the total precursor polymer). The fraction of pendant chains w_p is estimated from w_f by the equation: $w_p \cong 2p(1-p)$, where $p = w_f^{1/2}$ is the probability that an extremity of precursor chains did not react to contribute to a cross-link.[31] To measure the polymer volume fraction at swelling equilibrium Φ_e, we measured optically the dimension of a small rectangular sample, in the dry state and immersed in cyclohexane.

Φ_e is related to the average effective chain length N. The free energy per unit volume of the swollen network is (in k_BT units)[32]

$$f = (1-\Phi)\ln(1-\Phi) + \chi\Phi(1-\Phi) + \frac{3}{2}\frac{\Phi}{N}\frac{R^2}{{R_0}^2} \qquad (5)$$

Φ is the volume fraction occupied by network chains. For Gaussian chains, $R_0^2 = Na^2$ and at swelling equilibrium $\Phi = Na^3/R^3$ according to the c^* theorem.[32] Then the condition for equilibrium swelling $\Pi = 0$ (Π is the osmotic pressure) gives the equilibrium value

$$\Phi_e = a^{9/5}\nu^{-3/5}N^{-4/5} \qquad (6)$$

ν is the excluded volume parameter: $\nu = a^3(1-2\chi)$. For the PDMS/cyclohexane pair, $\chi = 0.42$.[33,34]

A series of bimodal networks was also studied, whose characteristics are summarized in Table 2.[21,35] They were synthesized from precursor chains of two different lengths. They are characterized by the volume fraction of long chains Φ_L. They were synthesized either with tetrakis(allyloxyethane) (index x) or with TVCS (index o). Either long or short chains are perdeuterated, allowing selective observation of either type of chains.

Table 2. Characteristics of Bimodal Networks[a]

refs	Φ_L	deuteriated chains
d^o	0.15	short
M^o	0.50	long
m^o	0.50	short
S^o	0.75	long
C^x	0.10	long
c^x	0.10	short
M^x	0.50	long
m^x	0.50	short

[a] Key: Φ_L, weight fraction of long precursor chains (M_n = 25 000); short precursor chains have M_n = 3000.

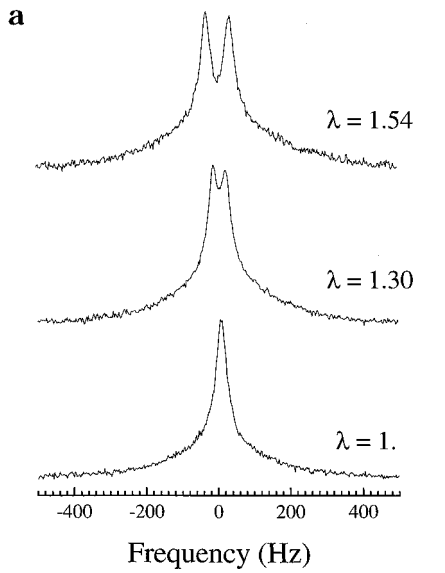

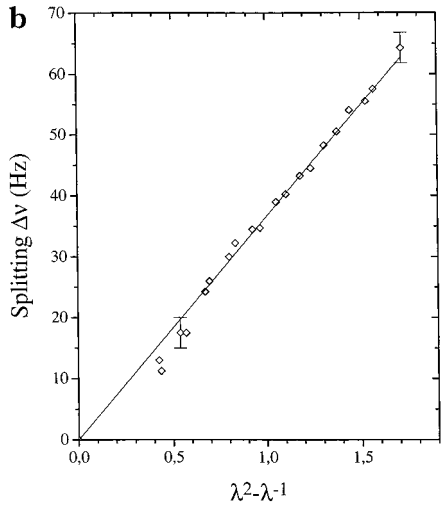

Figure 1. (a) Representative set of spectra obtained in network G21, at different elongation ratios λ. (b) NMR splitting $\Delta\nu$ plotted vs $\lambda^2 - \lambda^{-1}$. The slope P is obtained by a linear fit of the data.

3.2. NMR Experiments. Experiments were done at room temperature. To measure the slope P, samples were stretched uniaxially along the direction of the sample tube using a simple device described in ref 16. The elongation is measured optically with an accuracy of 0.2%. In this geometry the force is always perpendicular to the magnetic field, so that $|P_2(\Omega)| = {}^1/_2$ in eq 4. ^{2}H NMR experiments were done at 13 MHz on a Bruker CXP90 spectrometer. Figure 1a gives some representative examples of spectra for different elongation ratios λ, obtained in network G21. The corresponding splittings are plotted vs $\lambda^2 - \lambda^{-1}$ in Figure 1b, according to eq 4. Two methods were used to measure the relaxation function (or equivalently, the line shape). First, the envelope of the spin−

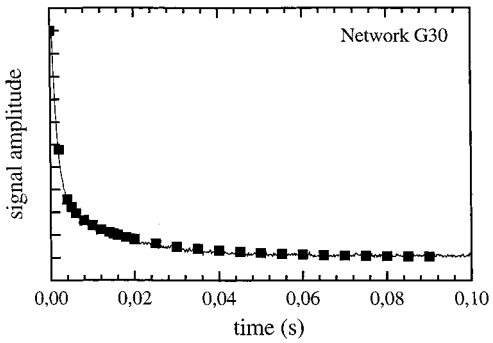

Figure 2. Free induction decay (FID) obtained in homogeneous field in network G30 (continuous line) compared to spin−echo maxima in a pulse sequence ($\pi/2$, $\pi(90°)$) (symbols). The spin−echo envelope superposes exactly the FID.

echo maxima in a simple ($\pi/2$, $\pi(90°)$) pulse sequence was recorded (90° is the phase of the second pulse). This was done on the CXP90 spectrometer. The time interval between pulses was varied between 200 μs and 50 ms. The $\pi/2$ pulse duration was about 7 μs. Another method is to record directly the free induction decay (FID), that is the relaxation signal after a single $\pi/2$ pulse, in a high resolution field. This was done at 36.1 MHz on a Bruker AM250 spectrometer. To obtain a highly homogeneous field within the samples, the network pieces (typically 1 × 4 × 5 mm) were immersed in a nondeuterated PDMS melt of length M_n = 25 000, and the field was shimmed carefully for each sample. The molten chains are longer than (or in some cases equal to) the average mesh size of the networks. Moreover, in each case the experiment was done immediately after immersion. This guarantees that the network does not swell in the melt,[36,37] and thus the network chains are not affected in this procedure. The field homogeneity was controlled by measuring the half-height line width of the proton signal, which comes mainly from the protonated melt (with a small contribution from the network). The line width is typically 10 to 12 Hz, which corresponds to a field inhomogeneity $\Delta B_0/B_0 \approx 0.05$ ppm at most in the entire volume of the sample. This gives a line broadening of 1.5−2 Hz at 36 MHz, which we consider to be negligible and is in any case comparable to the resolution of the spectra recorded. As an example, Figure 2 shows the FID (continuous line) and the spin−echo envelope for network G30. Both superpose exactly, which demonstrates that the effect of field inhomogeneity on the FID is negligible in the time range of observation of the signal. Solid echo train sequences were performed on the CXP90 spectrometer. The pulse sequence used is the OW4 sequence ($\pi/2$, (τ, $\pi/2(90°)$, τ)$_n$),[38,39] with values of τ between 200 μs and 4 ms. Special care was taken to obtain a homogeneous irradiation RF field. Other two-pulse sequences were performed on the CXP90 also.

4. Results

Table 3 gives a summary of all the measurements done (some of these numbers were already published[15−17,21]). It is clear, as was already mentionned before, that the "real" (chemical) chain length is not the only parameter which determines the properties of the networks. On one hand, networks with the same chain length distribution do not have the same measured parameters. On the other hand, networks with different chain lengths do have very close values.

4.1. Relation between Φ_e and P. Figure 3 shows the slope P, plotted as a function of Φ_e in monomodal networks. From eqs 4 and 6, we have (with $|P_2(\Omega)| = {}^1/_2$):

$$P = \frac{1}{5}\nu_Q \frac{u}{1-u}(1-2\chi)^{3/4}\Phi_e^{5/4} \qquad (7)$$

Table 3[a]

refs	slope P (Hz)	line width	Φ_e
G3	43	32.2	0.185[b]
G19	30.5		0.135[b]
G21	37.5	25.72	0.167[b]
G26	32.5	12.04	0.1[b]
G27	16.5	15.51	0.067[b]
G30	50	27.61	0.192
G31	40	39.12	0.152
G32	37.3		0.149
H21*	62.5	45.42	0.26
m^o	68.5[c]	70	
M^o	62[c]	53.68	
m^x	33[c]	28.37	
M^x	32[c]	24.37	
S^o	44[c]	30.37	
d^o	70[c]	29	
C^x	50[c]	19	
c^x	50[c]	18	

[a] Key: P, slope $\Delta\nu/(\lambda^2 - \lambda^{-1})$ where $\Delta\nu$ is the splitting measured at a elongation rate λ; Φ_e, the polymer network volume fraction at swelling equilibrium in cyclohexane. [b] From ref 17. [c] From ref 21.

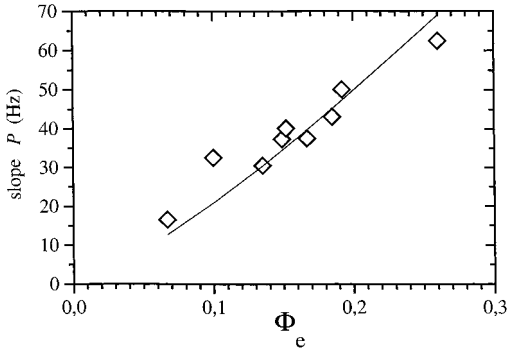

Figure 3. The slope $P = \Delta\nu/(\lambda^2 - \lambda^{-1})$ (see eq 7) plotted vs the polymer network volume fraction at swelling equilibrium Φ_e in the series of monomodal networks. The continuous line is the best fit using eq 11.

Figure 3 shows that there is indeed a clear correlation between P and Φ_e. The dispersion of the points and the rather limited range of accessible values does not allow to test eq 7, namely for instance the $^5/_4$ exponent. However, the fit shown in Figure 3 gives $P = 371.5\Phi_e^{5/4}$ (P measured in Hz), which gives the following value for the orientational interaction parameter u (in k_BT units):

$$u \cong 0.26 \tag{8}$$

This value is roughly consistent with that which may be extracted from similar data in ref 24. However, the PDMS networks described therein have slightly higher Φ_e's, which leads to a higher u ($u \cong 0.32$).

4.2. Relation between *P* and the Line Width. Figure 4 shows the slope P as a function of the half-height line width in the relaxed state, for different monomodal or bimodal networks. It appears immediately that there is no good correlation. However, we find that the slope and the half-height line width do have the same order of magnitude. The Gaussian model presented in section 2 may be used to relate quantitatively the line width to the effective chain length N. We calculate the function $M(t)$ given by eq 6 and then Fourier transform it and measure the half-height line width Δ on the resulting spectrum. One obtains the relation $\Delta \cong 4200/N$ (Δ measured in Hz). Then, the relation $\Delta \approx 0.67P$ (see Figure 4) gives $u = 0.6$. This value is significantly larger than the previous one.

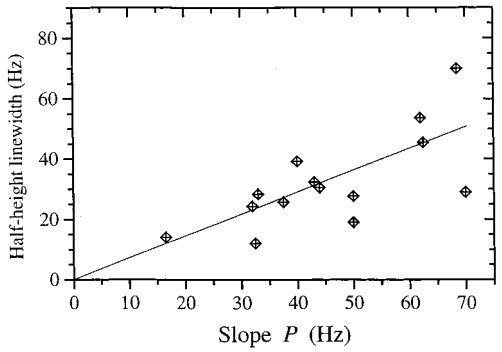

Figure 4. The slope P vs the half-height line width Δ in the relaxed state in the series of networks. The continuous line gives $\Delta = {}^2/_3P$.

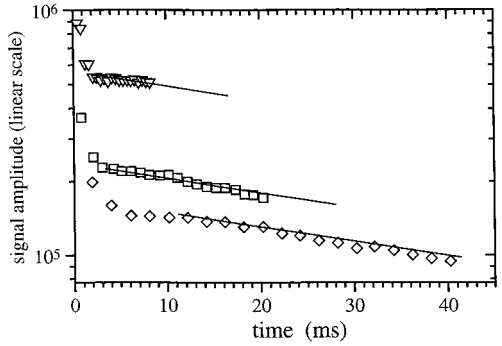

Figure 5. Solid echo maxima obtained in a OW4 sequence (see section 4.3.), in network H21, for three different values of the time interval τ between the pulses in the solid echo pulse train: (▽) $\tau = 0.2$ ms; (□) $\tau = 0.5$ ms; (◇) $\tau = 1$ ms.

4.3. Homogeneous vs Inhomogeneous Broadening. The result in section 4.2 suggests that the line width Δ and the slope P do not depend in the same way on the molecular parameters of the networks. It may be also that the parameter Δ alone is not appropriate to describe the line shape. Therefore the line shape has to be analyzed in a more detailed way.

The approach presented in Section 2, specifically eq 3, is based on two main assumptions.[5-9] First, anisotropic intrachain motions are fast with respect to the inverse line width. Then, the line shape itself is determined by the distribution of residual interactions. In other words, this means that the line shape is of inhomogeneous type.[26] This may be checked in several ways. This is specifically demonstrated by the appearance of a pseudo-solid echo.[5,7] Neglecting the homogeneous contribution to the line broadening requires estimating quantitatively the homogeneous (irreversible) contribution to the relaxation $\exp(-t/T_2)$, to estimate the ratio between homogeneous and inhomogeneous broadenings. This has been done by applying a solid echo pulse train using the OW4 sequence,[38,39] which refocuses quadrupolar residual interactions.[40-42] A solid echo is generated between each pair of $\pi/2$ pulses. Figure 5 shows the decays (amplitudes of the echo maxima) obtained in a solid echo train sequence, for three different values of the delay τ between the pulses. Resonance offsets and/or field inhomogeneities are only partially refocused in the OW4 sequence and part of the signal is lost at short time due to this effect.[9] This explains the difference in amplitude of the decays shown in Figure 5 for the different τ values. Indeed this difference depends on the resonance offset, which shows that this is not related to the presence of two compo-

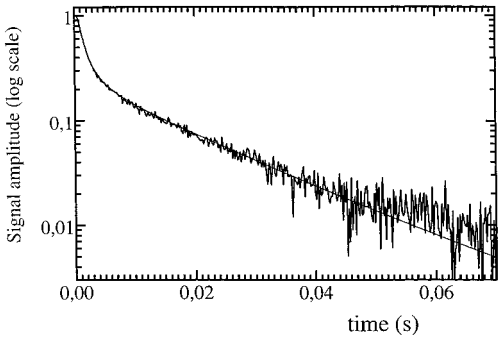

Figure 6. FID obtained in network G21, with amplitude in logarithmic scale. The fitting function is $M(t)$, given in eq 6 for the short time part, and is an exponential contribution at long times.

nents in the signal. The important point is that the decays are exponential after a few milliseconds, and that the relaxation time T_2^{eff} is practically independent of τ. This demonstrates that there is no contribution from slow motions in the relaxation (the correlation time τ_c is typically $\tau_c \leq 10^{-2}\tau$) or, in other words, that the system is in the fast motion regime. Fitting the long time part of the envelope of echo maxima with an exponential function gives a relaxation time T_2^{eff} of the order of 50−60 ms, depending on the network (it is 68 ms for network H21 which is shown in Figure 4). This value would correspond to a homogeneous broadening with a half-height line width $\Delta_{1/2} = 1/\pi T_2 \cong 5$ Hz. Thus, the ratio inhomogeneous/homogeneous broadening is not much larger than one, contrary to the case of a "true" solid. Strictly speaking, this would preclude neglecting the homogeneous contribution in the line width.

Then we have compared the relaxation functions obtained experimentally to the function $M(t)$ calculated within the Gaussian model in section 2. The fits obtained in this way are very poor in all cases, which indicates that the model does not provide a good representation of chain properties in the networks under study. One consequence of this is that resonance lines in the series of networks do not satisfy a superposition principle as expressed in eq 3. This could explain the dispersion of points in Figure 4.

4.4. Relaxation Functions in the PDMS Networks. The relaxation functions may be analyzed in two distinct contributions, one decreasing faster, at a short time, another one decreasing slower, at a longer time. Figure 6 shows the FID obtained in network G21. Data are fitted with a two-component fitting function. The function $M(t)$, eq 6, is used for the fast component and an exponential part is used for the slow component. Thus, three adjustable parameters are involved: the average residual interaction $\Delta = \omega_Q/5N$ (or equivalently the effective chain length N) in the fast part, the relaxation time T_2, and the relative fraction $(1 - \Phi)$ of the exponential tail. The values obtained from this fit are summarized in Table 4. Indeed, the two components behave in a different way. The pseudo-solid behavior (nonzero residual interactions) may be checked by comparing the echo envelopes obtained in the $(\pi/2, \tau, \pi(90°))$ and $(\pi/2, \tau, \pi/2(90°))$ pulse sequences, respectively.[5,8] The first one does not refocus quadrupolar interactions, and the obtained envelope $M_{\text{FID}}(t)$ is identical to the FID in homogeneous field (see Figure 2):

Table 4[a]

refs	Δ (rad·s^{-1})	Φ	T_2 (s)
G3	846	0.54	0.0189
G21	470	0.782	0.0229
G26	454	0.753	0.0344
G27	426	0.70	0.0265
G30	735	0.807	0.0173
G31	719	0.76	0.0112
H21	774	0.925	0.0251
m^x	1293	0.659	0.0176
M^x	681	0.6625	0.0238
S^o	788	0.78	0.0259
M^o	589	0.8	0.0133
m^o	1103	0.884	0.0073

[a] Key: Δ, average residual interaction $2\ 2\pi\nu_Q/5N$ measured from fitting the fast decaying (pseudo-solid) part of the FID; Φ, fraction of the pseudo-solid component in the FID; T_2, relaxation time of the liquid component in the FID.

$$M_{\text{FID}}(t) \cong \exp\left(-\frac{t}{T_2}\right)\langle\cos(\Delta_R t)\rangle \tag{9}$$

The latter one refocuses quadrupolar interactions, but only part of the field inhomogeneity; the envelope is denoted by $M_{\text{SE}}(t)$ and is given by (in inhomogeneous field):

$$M_{\text{SE}}(t) \cong \frac{1}{2}\exp\left(-\frac{t}{T_2}\right) \tag{10}$$

It was shown in section 4.3 (see also Figure 4) that the spin−echo envelope is roughly exponential. This allows one to extract the T_2 term from the ensemble average as it is done in eq 10, to a good approximation. Then the ratio

$$Q(t) = \frac{M_{\text{FID}}(t)}{2M_{\text{SE}}(t)} \cong \langle\cos(\Delta_R t)\rangle \tag{11}$$

allows one to isolate the contribution from residual interactions. The ratio $Q(t)$ measured in network G30 is plotted in Figure 7. To increase the precision at long times, $Q(t)$ was determined for each time t_0 by fitting the complete expression for the spin−echo maximum in a pulse sequence $(\pi/2, \tau, \beta(90°))$[43]

$$M_\beta(t_0) \cong \frac{1}{2}[\sin^2\beta - \cos\beta\,(1 - \cos\beta)Q(t_0)] \tag{12}$$

The length β of the second pulse (measured in degrees) was varied between $\pi/10$ and π, by steps of $\pi/10$, typically. It is observed that the ratio $Q(t)$ does not decrease to zero, but reaches a constant value after a characteristic time of the order 10 ms. Within experimental uncertainties, this value is the same as the fraction of the slow, exponential component introduced in the composite fit in Figure 6. The relaxation time T_2^{slow} of the slow component is of the order 10 to 35 ms depending on the network. This is shorter than the values for T_2^{eff} measured above. This suggests that slow motions may contribute to this part of the signal. Indeed, in the limit of fast motions, one would expect T_2^{slow} to be equal to T_2^{eff}.[40,41] Anyway, this contribution is perceived as a liquidlike component, without permanent residual interactions. T_2^{slow} as well as T_2^{eff} is shorter than the transverse relaxation time in the corresponding melt, which is a pure liquid from the

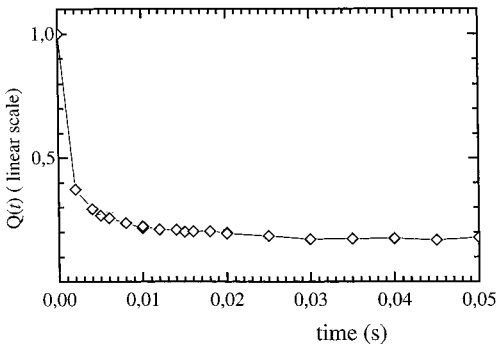

Figure 7. The ratio $Q(t)$ of the echo amplitudes in the (π/2, π) and (π/2, π/2) pulse sequences respectively, in network G30.

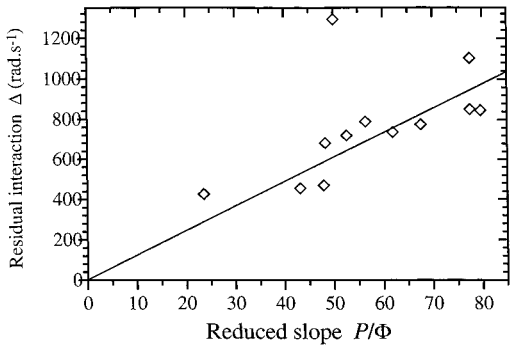

Figure 8. The residual interaction $\Delta = 2\pi\nu_Q/5N$ (see eq 6) measured in rad·s^{-1}, estimated from fitting the fast, pseudo-solid component in the relaxation signal, plotted as a function of the reduced slope P/Φ measured in Hz. Φ is the liquid fraction, i.e., the fraction of the slow, liquidlike part of the signal. The continuous line gives $P/\Phi = 0.08\Delta$.

NMR point of view: a PDMS melt of chain length $M_n = 6000$ has T_2 equal to 180 ms at room temperature.

5. Discussion

The results presented above confirm that the signal in PDMS networks may be analyzed in two components.[13,44−46] This was already observed by ^{1}H NMR in similar PDMS networks.[47] The component relaxing slower may be clearly attributed to dangling chains, as shown in ref 24. The liquid fraction ($1 - \Phi$) (see Table 4) has to be compared to the estimated fraction of dangling chains w_p (Table 1). The correlation between both quantities is difficult to establish. It is observed generally (except in one case) that ($1 - \Phi$) is larger than w_p. This would suggest that other defects, such as closed loops, may contribute also to the liquid fraction. Additionally, the fraction of dangling chains calculated from w_f may be underestimated. We suggest here that NMR may provide a way to measure accurately the fraction of dangling chains, which is often not controlled in network samples.

It is interesting to compare the obtained N values to the actual chemical length of presursor chains. It is generally admitted that a statistical segment in the PDMS chain corresponds to six backbone bonds, that is, to three monomers.[48] An average residual interaction as defined in eq 3 $\Delta = \omega_Q/5N \cong 700$ rad·s^{-1} (see Table 4) corresponds to an average chain length $N = \omega_Q/5\Delta \cong 36$ statistical segments, that is, to about 110 monomers. Chains with $M_n = 10000$ have about 135 monomers on average. Both values are thus roughly consistent with each other. Therefore, no evidence for a direct effect of trapped entanglements is obtained in that way.

We demonstrate here that elastic chains and dangling chains have qualitatively different NMR behaviors. Whereas elastic chains are pseudo-solids, dangling chains are purely liquid in the relaxed state, which indicates that they are free to reorient isotropically on the NMR time scale. This confirms that NMR properties are essentially determined by the constraints exerted on the chains, which either prevent (for elastic chains) or allow (for dangling chains) isotropic reorientation. Thus, the two populations differ in the statistical properties of chains, rather than in the time scale of the motions. From that point of view, dangling chains behave in a way similar to free chains, and they orient on stretching the networks.

The presence of a liquid fraction should be taken into account in the description of the permanent orientational order induced upon stretching. In the mean field model developped previously,[20,49] the complete expression for the residual quadrupolar interaction in a network chain is[20]

$$\Delta_{\vec{R}} = \omega_Q\left[\frac{3}{5}\frac{R^2}{N^2a^2}P_2(\alpha) + \frac{1}{5}\frac{u}{1-u}\frac{1}{N}(\lambda^2 - \lambda^1)P_2(\Omega)\right] \quad (13)$$

The residual interaction tensor includes a term averaged along the end-to-end vector (first term in (13)) and a uniaxial, mean-field term, averaged along the applied external force (second term in (13)). For free chains, only that latter term is present.[20] Then, if only a fraction Φ of the network chains are effectively elastic, i.e., are submitted to the constraints on extremities which lead to the first term in eq 13, the residual interaction has to be rewritten:[50]

$$\Delta_{\vec{R}} = \omega_Q\left[\frac{3}{5}\frac{R^2}{N^2a^2}P_2(\alpha) + \frac{1}{5}\frac{u}{1-u}\frac{\Phi}{N}(\lambda^2 - \lambda^1)P_2(\Omega)\right] \quad (14)$$

The first term in eq 14, related to entropic elasticity of chains, is considered to be unaffected. In other words, the distribution of interactions in elastic chains is the same as it would be in the absence of a liquid fraction in the signal. The splitting induced upon stretching comes from the second (uniaxial) term (it is equal to twice the interaction). Thus the slope P is weighted by a factor Φ. Then the quantities to compare are P/Φ and the magnitude of residual interactions in the pseudo-solid part of the signal, coming from elastic chains. In Figure 8, the residual interaction $\Delta = 2\pi\nu_Q/5N$ is plotted as a function of the reduced slope P/Φ for different networks. The correlation is significantly better than in Figure 4, both for monomodal and bimodal networks, except for one point. The corresponding sample is not perfectly transparent, which may be due to heterogeneities in the cross-link density. Two other samples are not reported in Figure 8 for the same reason. From Figure 8, the following relationship is obtained:

$$\frac{P}{\Phi} \cong 0.08\ \Delta \quad (15)$$

This gives the value

$$u \cong 0.33 \quad (16)$$

The agreement with the estimate given in section 4.1 is good, given the rather large error bars in the

measurements presented in Figure 8. The values given here are consistent with those estimated from previous measurements.[18−20] It was shown also that Monte Carlo simulations give very similar values for u.[51,52]

The orientation of probe molecules and/or free chains was used to estimate the coupling constant u. Specifically, the ratio ϵ of probe orientation to network chain orientation was measured with various techniques. Whereas NMR experiments generally give $\epsilon = 1$ when probe chains identical to network chains are used,[18,53] other techniques give ϵ between 0.3 and 0.7 depending on the system.[54−56] Related to this apparent contradiction, there has been a controversy on the interpretation of the coupling constant u. An alternative explanation was proposed to account for this discrepancy, based on a distribution of motional rates in the system.[57] Dangling chains were supposed to contribute to the narrow component in the spectrum, that is, to move faster. Here we assign the narrow components in the spectra to dangling chains as well. However, the mean field effect described by eq 13 and 14 is sufficient to model the orientational behavior. Indeed, the doublets for both network and dangling (or free) chains are measured by the second term in eq 14. This gives an orientation for free chains, along the stretching direction (in the limit of infinite free chain dilution) given by the order parameter

$$S_F = \frac{1}{5N}\frac{u}{1-u}(\lambda^2 - \lambda^{-1}) \qquad (17)$$

The *average* orientation $\langle S_0 \rangle$ of network chain segments is measured in optical techniques. It is given by a self-consistent equation which leads to

$$\langle S_0 \rangle = \frac{1}{5N}\frac{1}{1-u}(\lambda^2 - \lambda^{-1}) \qquad (18)$$

Thus the ratio $\epsilon = S_F/\langle S_0 \rangle = u$, even though the same doublet is measured in free and network chains in NMR. This peculiar NMR observation is related to the symmetry of the mean orientational field in the stretched system, with no need to invoke dynamic heterogeneities. An alternative theory was also proposed, based on isotropic excluded volume interactions.[58] An interpretation of the parameter u in terms of the Edwards screening length ξ was given. That theory is consistent with the present results, since it takes into account explicitly the uniaxial symmetry of the stretched system.

6. Conclusion

We have studied a series of PDMS end-linked networks, with different molecular characteristics, namely precursor chain length, functionnality and chemical nature of cross-link junctions, density of trapped entanglements, and chain length distribution (monomodal or bimodal). Three quantities were measured independently: the magnitude of residual interactions in the relaxed state Δ, the slope P, i.e., the magnitude of the orientation induced upon stretching, and the polymer volume fraction at swelling equilibrium in a good solvent Φ_e. All these three quantities are related to an effective average chain length N.

A number of difficulties remain for a quantitative analysis of the present measurements:

(1) The local order, i.e., the average orientation, is probably not uniform along the chains. Chain extremities (close to cross-link junctions) may be more oriented than central fragments.[45]

(2) the chain length is rather broadly distributed (polydispersity index 1.6).

(3) cross-link fluctuations, as well as heterogeneities in the cross-link density, are not properly taken into account.

However, we could demonstrate that all three quantities correlate well, provided that a fraction of liquid component in the NMR signal is taken into account. This component is attributed to dangling chains. A step further is achieved when comparing the number values obtained for the different measured quantities. The values are consistent with molecular characteristics of the networks and give a coherent estimate of the parameter u ($u \cong 0.3$), which measures the strength of short-range orientational interactions. This reinforce the physical basis for the model of orientational interactions[20] which has been proposed to interpret the uniaxial order induced upon stretching.

References and Notes

(1) McCrum, N. G.; Buckley, C. P.; Bucknall, C. B. *Principles of Polymer Engineering*; Oxford Science Publications: Oxford University Press: Oxford, England 1994.
(2) Koenig, J. L. *Spectroscopy of Polymers*; ACS Professional Reference Book; American Chemical Society: Washington, DC, 1992.
(3) Mark, J. E.; Erman, B. *Rubber-like Elasticity, a molecular primer*, Wiley-Interscience: New York, 1988.
(4) *Physical Properties of Polymeric Gels*; Cohen-Addad, J. P., Ed.; John Wiley & Sons: Chichester, England, 1996.
(5) Cohen-Addad, J. P. NMR and Fractal Properties of Polymeric Liquids and Gels. In *Progress in NMR Spectroscopy*; Emsley, J. W., Feeney, J., Sutcliffe, L. H., Eds.; Pergamon Press: Oxford, England 1993.
(6) Fedotov, V. D.; Schneider, H. Structure and Dynamics of Bulk Polymers by NMR Method. In *NMR, Basic Principles and Progress*; Springer: Berlin, 1989; Vol. 21.
(7) Cohen-Addad, J. P.; Vogin, R. *Phys. Rev. Lett.* **1974**, *33*, 940.
(8) Cohen-Addad, J. P. *J. Chem. Phys.* **1974**, *60*, 2440.
(9) Sotta, P.; Fuelber, C.; Demco, D.; Bluemich, B.; Spiess, H. W. *Macromolecules* **1996**, *29*, 6222.
(10) Collignon, J.; Sillescu, H.; Spiess, H. W. *Colloid Polym. Sci.* **1981**, *259*, 220.
(11) Spiess, H. W. *Colloid Polym. Sci.* **1983**, *261*, 193.
(12) Lifchits, M. I. *Polymer* **1987**, *28*, 454.
(13) Cohen-Addad, J. P.; Dupeyre, R. *Polymer* **1983**, *24*, 400.
(14) Deloche, B.; Samulski, E. T. *Macromolecules* **1981**, *14*, 575.
(15) Dubault, A.; Deloche, B.; Herz, J. *Polymer* **1984**, *25*, 1405.
(16) Deloche, B.; Dubault, A.; Herz, J. *Europhys. Lett.* **1986**, *1*, 629.
(17) Dubault, A.; Deloche, B.; Herz, J. *Macromolecules* **1987**, *20*, 2096.
(18) Sotta, P.; Deloche, B.; Herz, J.; Lapp, A.; Durand, D.; Rabadeux, J. C. *Macromolecules* **1987**, *20*, 2769.
(19) Sotta, P.; Deloche, B.; Herz. J. *Polymer* **1988**, *29*, 1171.
(20) Sotta, P.; Deloche, B. *Macromolecules* **1990**, *23*, 1999.
(21) Chapellier, B.; Deloche, B.; Oeser, R. *J. Phys. II* **1993**, *3*, 1619.
(22) Klinkenberg, M.; Blümler, P.; Blümich, B. *Macromolecules* **1997**, *30*, 1038.
(23) McLoughlin, K.; Waldbieser, J. K.; Cohen, C.; Duncan, T. M. *Macromolecules* **1997**, *30*, 1044.
(24) McLoughlin, K.; Szeto, C.; Duncan, T. M.; Cohen, C. *Macromolecules* **1996**, *29*, 5475.
(25) Samulski, E. T. *Polymer* **1985**, *26*, 177 and references therein.
(26) Schmidt-Rohr, K.; Spiess, H. W. *Multidimensional Solid-State NMR and Polymers*, Academic Press: London, 1994.
(27) English, A. D. *Macromolecules* **1985**, *18*, 179.
(28) Schneider, B.; Doskocilova, D.; Dybal, J. *Polymer* **1985**, *26*, 253.
(29) Herz, J.; Belkebir, A.; Rempp, P. *Eur. Polym. J.* **1973**, *9*, 1165.
(30) Beltzung, M.; Picot, C.; Rempp. P. *Macromolecules* **1982**, *15*, 1594.
(31) Miller, D. R.; Macosko, C. W. *Macromolecules* **1976**, *9*, 206.
(32) De Gennes, P. G. *Scaling Concepts in Polymer Physics*, Cornell University Press: Ithaca, New York 1979.

(33) Flory, P. J. *Discuss. Faraday Soc.* **1970**, *49*, 7.
(34) Kuwahara, N.; Okazawa, T.; Kaneko, M. *Polym. Sci.* **1968**, *C23*, 543.
(35) Oeser, R. Ph.D. Thesis, University of Mainz 1992.
(36) Brochard, F. *J. Phys. (Paris)* **1981**, *42*, 505.
(37) Garrido, L.; Mark, J. E.; Clarson, S.; Semlyen, J. A. *Polymer* **1984**, *25*, 218.
(38) Ostroff, E. D.; Waugh, J. S. *Phys. Rev. Lett.* **1966**, *16*, 1097.
(39) Mansfield, P.; Ware, D. *Phys. Rev.* **1968**, *168*, 318.
(40) Schmiedel, H.; Freude, D.; Gründer, W. *Phys. Lett.* **1971**, *34A*, 162.
(41) Ursu, I.; Balibanu, F.; Demco, D. E.; Bogdan, M. *Phys. Status Solidi* **1986**, *136*, 309.
(42) Cohen-Addad, J. P.; Guillermo, A.; Lartigue, C. *Phys. Rev. Lett.* **1995**, *74*, 3820.
(43) Charvolin, J.; Rigny, P. *C. R. Acad. Sci. Paris* **1969**, *B269*, 224.
(44) Cohen-Addad, J. P. *J. Chem. Phys.* **1976**, *64*, 3438.
(45) Gronski, W.; Stadler, R.; Jacobi, M. M. *Macromolecules* **1984**, *17*, 741.
(46) Simon, G.; Baumann, K.; Gronski, W. *Macromolecules* **1992**, *25*, 3624.
(47) Simon, G.; Birnstiel, A.; Schimmel, K. H. *Polym. Bull.* **1989**, *21*, 235.
(48) Aharoni, S. *Macromolecules* **1983**, *16*, 1722.
(49) Jarry, J. P.; Monnerie, L. *Macromolecules* **1979**, *12*, 316.
(50) Sotta, P. In *Trends in Macromolecular Research*; The Council of Scientific Integration: India, 1994.
(51) Depner, M.; Deloche, B.; Sotta, P. *Macromolecules* **1994**, *27*, 5192.
(52) Sotta, P.; Higgs, P. G.; Depner, M.; Deloche, B. *Macromolecules* **1995**, *28*, 7208.
(53) Jacobi, M. M.; Stadler, R.; Gronski, W. *Macromolecules* **1986**, *19*, 2884.
(54) Jarry, J. P.; Monnerie, L. *J. Polym. Sci., Polym. Phys. Ed.* **1978**, *16*, 443.
(55) Kornfield, J. A.; Fuller, G. G.; Pearson, D. S. *Macromolecules* **1989**, *22*, 1334.
(56) Seidel, U.; Stadler, R.; Fuller, G. G. *Macromolecules* **1995**, *28*, 3739.
(57) Kornfiel, J. A.; Geun-Chang Chung; Smith, S. D. *Macromolecules* **1992**, *25*, 4442.
(58) Brereton, M. G. *Macromolecules* **1993**, *26*, 1152.

MA970994M